CT Features of COVID-19 Pneumonia Differ Depending on the Severity and Duration of Disease

Veränderung der CT-Morphologie bei COVID-19-Pneumonie, abhängig von Schwere und Dauer der Erkrankung

Authors

Jan Schaible[1], Stefanie Meiler[1], Florian Poschenrieder[1], Gregor Scharf[1], Florian Zeman[2], Charlotte Knobloch[1], Janine Rennert[1], Benedikt Pregler[1], Henning Kleine[3], Cynthia Menzel[4], Christian Stroszczynski[1], Niels Zorger[4], Okka W Hamer[1, 5]

Affiliations

1 Regensburg University Medical Center, Department of Radiology, Regensburg, Germany
2 Regensburg University Medical Center, Center for Clinical Studies, Regensburg, Germany
3 Hospital Barmherzige Brüder, Department of Pneumology, Regensburg, Germany
4 Hospital Barmherzige Brüder, Department of Radiology, Regensburg, Germany
5 Hospital Donaustauf, Department of Radiology, Donaustauf, Germany

Key words

COVID-19 pneumonia, CT, morphology, severity, duration

received 26.05.2020
accepted 11.10.2020
published online 17.12.2020

Bibliography

Fortschr Röntgenstr 2021; 193: 672–682
DOI 10.1055/a-1293-9163
ISSN 1438-9029

Georg Thieme Verlag KG, Rüdigerstraße 14, 70469 Stuttgart, Germany

Correspondence

Dr. Jan Schaible
Regensburg University Medical Center, Department of Radiology, Franz-Josef-Strauß-Allee 11, 93053 Regensburg, Germany
Tel.: +49/9 41/94 41 74 62
jan.schaible@ukr.de

ZUSAMMENFASSUNG

Hintergrund Die CT ist ein wichtiger Bestandteil bei der Versorgung von Patienten mit COVID-19-Pneumonie. Allerdings kann sich die CT-Morphologie stark verändern. Ziel dieser Studie war die Evaluation der CT-Morphologie von mittels RT-PCR nachgewiesenen COVID-19-Pneumonien in einer Kohorte aus Deutschland mit besonderem Augenmerk auf Veränderungen der CT-Muster in Abhängigkeit von Dauer und Schwere der Erkrankung.

Methodik Alle Patienten, bei denen zwischen dem 1. März und 15. April 2020 mittels RT-PCR eine COVID-19-Pneumonie nachgewiesen wurde und die eine Thorax-CT erhalten hatten, wurden retrospektiv identifiziert. Die Thorax-CTs wurden nach folgenden Kriterien ausgewertet: Vorhandensein verschiedener CT-Zeichen (z. B. Milchglas, Konsolidierung etc.), Verteilung und Ausmaß innerhalb der Lunge. Für die Subgruppenanalyse wurden die Patienten anhand des Ausmaßes der Lungenbeteiligung (0–33 %, 34–66 %, 67–100 %) und anhand des Zeitintervalls zwischen Symptombeginn und CT-Untersuchung (0–5 d, 6–10 d, 11–15 d, > 15 d) eingeteilt. Für die statistische Analyse wurde der Mantel-Haenszel-Test verwendet.

Ergebnisse Sowohl die Häufigkeit der CT-Zeichen (Milchglas, Konsolidierung, crazy paving, bronchiale Dilatationen, Gefäßerweiterung, Lymphadenopathie, Pleuraerguss) als auch die Verteilung innerhalb der Lunge waren je nach Dauer und Ausmaß der Erkrankung signifikant unterschiedlich. Die Frühphase der Erkrankung war vor allem durch Milchglas und weniger durch Konsolidierungen charakterisiert. Die Verdichtungen zeigten häufig eine runde Form und waren anteilig scharf berandet oder geografisch konfiguriert. Die Gefäße innerhalb oder in der Nähe der Verdichtungen waren häufig erweitert. Im weiteren Verlauf nahmen die Konsolidierungen und das crazy paving zu. Die runde oder geografische Form nahm an Häufigkeit ab. Nach dem 15. Tag traten bronchiale Dilatationen auf, und eine Lymphadenopathie und Pleuraergüsse wurden häufiger als zuvor beobachtet.

Schlussfolgerung Die CT-Muster variierten in Abhängigkeit von Krankheitsdauer und Schwere der Erkrankung. Daher sollten Radiologen sowohl das Zeitintervall zwischen Symptombeginn und CT-Datum als auch die Schwere der Erkrankung berücksichtigen, wenn differenzialdiagnostisch eine COVID-19-Pneumonie diskutiert wird.

Kernaussagen:

- Die Häufigkeit der CT-Zeichen und die Verteilung innerhalb der Lunge variieren abhängig von Dauer und Schwere der COVID-19-Pneumonie.
- Die Frühphase ist durch Milchglas und Konsolidierungen charakterisiert, die häufig eine runde Form zeigen und

zumindest teilweise scharf berandet oder geografisch konfiguriert sind.
- Die Häufigkeit von Konsolidierungen und vor allem des crazy pavings nimmt mit zunehmender Dauer der Erkrankung zu
- In der Spätphase (> 15 Tage nach Symptombeginn) treten bronchiale Dilatationen auf.
- Radiologen sollten Dauer und Schwere der Erkrankung berücksichtigen, wenn differenzialdiagnostisch eine COVID-19-Pneumonie diskutiert wird.

ABSTRACT

Background CT is important in the care of patients with COVID-19 pneumonia. However, CT morphology can change significantly over the course of the disease. To evaluate the CT morphology of RT-PCR-proven COVID-19 pneumonia in a German cohort with special emphasis on identification of potential differences of CT features depending on duration and severity of disease.

Method All patients with RT-PCR-proven COVID-19 pneumonia and chest CT performed between March 1 and April 15, 2020 were retrospectively identified. The CT scans were evaluated regarding the presence of different CT features (e. g. ground glass opacity, consolidation, crazy paving, vessel enlargement, shape, and margin of opacifications), distribution of lesions in the lung and extent of parenchymal involvement. For subgroup analyses the patients were divided according to the percentage of parenchymal opacification (0–33 %, 34–66 %, 67–100 %) and according to time interval between symptom onset and CT date (0–5 d, 6–10 d, 11–15 d, > 15 d). Differences in CT features and distribution between subgroups were tested using the Mantel-Haenszel Chi Squared for trend.

Results The frequency of CT features (ground glass opacity, consolidation, crazy paving, bronchial dilatation, vessel enlargement, lymphadenopathy, pleural effusion) as well as pattern of parenchymal involvement differed significantly depending on the duration of disease and extent of parenchymal involvement. The early phase of disease was characterized by GGO and to a lesser extent consolidation. The opacifications tended to be round and to some extent with sharp margins and a geographic configuration. The vessels within/around the opacifications were frequently dilated. Later on, the frequency of consolidation and especially crazy paving increased, and the round/geographic shape faded. After day 15, bronchial dilatation occurred, and lymphadenopathy and pleural effusion were seen more frequently than before.

Conclusion The prevalence of CT features varied considerably during the course of disease and depending on the severity of parenchymal involvement. Radiologists should take into account the time interval between symptom onset and date of CT and the severity of disease when discussing the likelihood of COVID-19 pneumonia based on CT morphology.

Key Points:
- The frequency of CT features and pattern of parenchymal involvement vary depending on the duration and extent of COVID-19 pneumonia.
- The early phase is characterized by GGO and consolidation which demonstrate a round shape and at least to some extent have sharp margins and a geographic configuration.
- The frequency of consolidation and especially crazy paving increases during the course of disease.
- Beyond day 15 after symptom onset, bronchial dilatation occurs.
- Radiologists should take into account the duration and severity of disease when considering COVID-19 pneumonia.

Citation Format
- Schaible J, Meiler S, Poschenrieder F et al. CT Features of COVID-19 Pneumonia Differ Depending on the Severity and Duration of Disease. Fortschr Röntgenstr 2021; 193: 672–682

Introduction

Since the outbreak of coronavirus disease 2019 (COVID-19) in December 2019, several studies reporting the morphology of COVID-19 pneumonia on chest computed tomography (CT) have been published [1–5]. Most studies are from Chinese cohorts because the disease first appeared in Wuhan, China before becoming a pandemic. At present, European studies are still scarce [6]. However, CT morphology might be affected by host features that are not only influenced by individual factors but also by ethnicity. Moreover, viral genome variability due to constantly occurring mutations might change imaging features. Hence, it is worthwhile to analyze the CT morphology in a European cohort.

Unlike in most other viral pneumonias, the CT morphology of COVID-19 pneumonia seems to exhibit remarkably similar features in many patients. This circumstance has triggered the development of assessment and reporting schemes categorizing the CT findings into different groups of likelihood for COVID-19 pneumonia [7–9]. Nevertheless, the specificity of CT for COVID-19 pneumonia is reported to be as low as 37 % [10]. Obviously, the specificity is hampered by morphologic similarities to other types of pneumonias and sterile pneumonitis. Additional factors limiting specificity might be on the one hand a potential variability of the "faces" of COVID-19 pneumonia depending on the time interval between symptom onset and acquisition of images and on the other hand depending on the severity of disease.

The aim of this study was to evaluate the CT morphology of reverse transcription polymerase chain reaction-proven (RT-PCR) COVID-19 pneumonia in a German cohort with special emphasis on the identification of potential differences of CT features depending on the duration and severity of disease.

Material and Methods

Patient population

This retrospective study was approved by the institutional ethics committee. All procedures performed in studies involving human participants were in accordance with the ethical standards of the institutional and/or national research committee and with the 1964 Helsinki declaration and its later amendments or comparable ethical standards. Written informed consent was waived.

The inclusion criteria were consecutive adult patients (≥ 18 years old) with RT-PCR positive for Severe Acute Respiratory Syndrome Coronavirus 2 (SARS-CoV-2) and a chest CT performed between March 1 and April 15, 2020. The exclusion criteria were a negative result of RT-PCR for SARS-CoV-2 and non-diagnostic CT, for example due to motion artifacts. Patients were identified by means of a full-text database query of all CT scans performed between March 1, and April 15, 2020 using the term "*COVID*" and *SARS* in the Radiological Information System (RIS, Nexus.medRIS, Version 8.42, Nexus, Villingen-Schwenningen, Germany). Patient characteristics (age, gender, comorbidities), symptoms, date of symptom onset and RT-PCR results were extracted from electronic patient records. All patients had at least one CT scan of the chest. 5 patients had two scans, 2 patients had three scans and 1 patient had four scans. Thus, 120 CT scans were included in the study. Follow-up CT scans were at least 5 days apart (5 days n = 1, 7 days n = 2, 8 days n = 2, 9 days n = 3, 10 days n = 1, 12 days n = 1, 18 days n = 1, 25 days n = 1).

CT protocol

The patients underwent CT scans at two tertiary care hospitals. Chest CT scans were acquired on two different scanners (16 slice Somatom Sensation 16, 128-slice Definition FLASH, both Siemens Healthcare, Erlangen, Germany). All CT acquisitions were obtained in supine position during end-inspiration. Intravenous contrast material was administered at the discretion of the radiologist considering the individual study indication. Automatic tube voltage selection was applied with a reference tube voltage of 120 kV. Tube current was regulated by an automatic tube current modulation technique with the reference mAs being 40–110. The collimation width was 0.625–0.75 mm. Multiplanar reformations (MPRs) were reconstructed in the axial plane with a slice thickness of 0.75–1.5 mm (108 CT scans) and 3–4 mm (12 CT scans) in the lung kernel and with a slice thickness of 1–5 mm in the soft tissue kernel. Additional sagittal and coronal MPRs were reconstructed with a slice thickness of 1–3 mm using the lung and soft tissue kernels. The pictures were sent to a picture archiving and communication system (PACS, Syngo Imaging, Siemens, Erlangen, Germany).

Image analysis

Before the study cases were read, all features were explicitly discussed in example cases which were not part of the study. Two radiologists with subspeciality training in thoracic radiology evaluated each half of the CT studies on a PACS workstation (Syngo Imaging, Siemens, Erlangen, Germany). In equivocal cases a senior thoracic radiologist was consulted, and the respective case was read in consensus. The radiologists were blinded to clinical data, laboratory data, and patient status. The Fleischner Society definition of CT features was applied when appropriate. The following parameters were analyzed:

- Ground-glass opacities (GGO): hazy increased opacity of lung, with preservation of bronchial and vascular margins.
- Consolidation: homogeneous increase in pulmonary parenchymal attenuation that obscures the margins of vessels and airway walls
- Crazy paving pattern: thickened interlobular septa and intralobular lines superimposed on a background of ground-glass opacity.
- Nodule: rounded opacity, with sharp or unsharp margins, measuring up to 3 cm in diameter.
- Cavity: gas-filled space within consolidation
- Bronchial dilatation: dilated (with respect to the accompanying pulmonary artery) non-tapering bronchus. The term "dilatation" instead of "ectasis" was intentionally used in order to express that the pathology might be reversible.
- Vessel dilatation: diameter of vessel within or near opacifications clearly larger compared to vessels of the same generation in healthy lung tissue.
- Shape of opacification: round, curvilinear/band-like, geographic (= opacification outlines the shape of multiple adjacent pulmonary lobules, sharply marginated)
- Margin of opacification: unsharp, at least to some extent sharp
- Lung lobes affected
- Distribution of opacifications in the axial plane: predominantly peripheral, predominantly central, predominantly anterior, predominantly posterior, diffuse
- Lymphadenopathy: diameter > 10 mm in the short axis
- Subjective estimation of extent of parenchymal opacification: 0–33 %: mild, 34–66 %: moderate, 67–100 %: severe (▶ **Fig. 1**)

Statistical Analysis

Statistical analysis was performed using R, version 3.6.1 (The R Foundation for Statistical Computing). All continuous variables were expressed as medians and ranges and categorical variables as count and percentages.

For subgroup analyses the patients were divided according to the amount of parenchymal opacification and according to the time interval between symptom onset and CT date using the Mantel-Haenszel Chi Squared for trend.

Results

Patient population and clinical symptoms

The study population consisted of 108 patients (64 men = 59 %) with a mean age of 59.6 (SD 13.8). Clinical symptoms were fever in 74 patients (69 %), cough in 86 patients (80 %), dyspnea in 63 patients (58 %) and fatigue in 52 patients (48 %). Less frequently seen were gastrointestinal complaints (n = 22; 20 %) and taste dysfunction (n = 20; 19 %). The results are presented in ▶ **Table 1**.

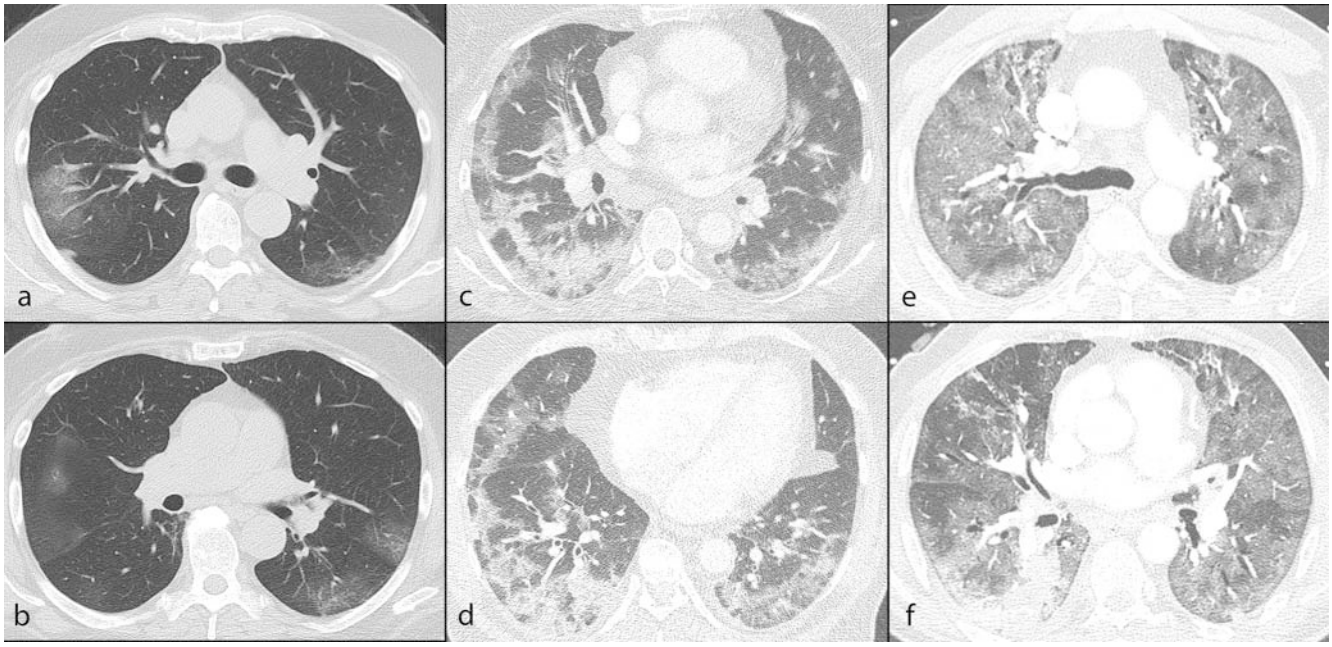

▶ **Fig. 1** Extent of parenchymal involvement. Axial MPRs in two different slice positions of thin-section CT scans of three patients with RT-PCR-proven COVID-19 pneumonia. **a, b** CT demonstrates a mild extent of parenchymal opacifications (< 33 % of lung tissue volume). Several roundish ground glass opacities in the periphery of the posterior lung segments are identifiable. **c, d** CT demonstrates a moderate extent of parenchymal opacifications (34–66 % of lung tissue volume). Confluent consolidation and ground glass opacities in the periphery of both lungs. Some of the opacifications have sharp margins and a geographic configuration. **e, f** CT demonstrates a severe extent of parenchymal opacifications (> 66 % of lung tissue volume). Consolidation and crazy paving are diffusely distributed in both lungs. Some bronchi are dilated.

▶ **Abb. 1** Ausmaß der parenchymalen Beteiligung. Axiale MPRs an zwei verschiedenen Schichtpositionen von Dünnschicht-CT-Scans dreier Patienten mit RT-PCR gesicherter COVID-19-Pneumonie. **a, b** Die CT zeigt ein mildes Ausmaß der Verdichtungen (< 33 % des Lungenvolumens). Mehrere rundliche Milchglastrübungen lassen sich in der Peripherie der dorsalen Lungensegmente erkennen. **c, d** Die CT zeigt ein mäßiges Ausmaß der Verdichtungen (34–66 % des Lungenvolumens). Konfluierende Konsolidierungen und Milchglas in der Peripherie beider Lungen. Einige Verdichtungen zeigen eine scharfe Berandung und eine geographische Konfiguration. **e, f** Die CT zeigt ein schweres Ausmaß der Verdichtungen (> 66 % des Lungenvolumens). Konsolidierung und sog. „crazy paving" sind in beiden Lungenflügeln diffus verteilt. Einige Bronchien sind dilatiert.

▶ **Table 1** Patient characteristics (n = 108).

	n	%
mean age	59.6 (SD 13.8)	
male	64	59
fever (> 37.5 °C)	74	69
cough	86	80
dyspnea	63	58
fatigue	52	48
gastrointestinal complaints	22	20
dysfunction of taste	20	19

CT morphology

Total study group

The time interval between symptom onset and CT examination (first CT scan in case more than one was acquired) was mean 14.9 days (minimum 1 d, maximum 40 d, SD 37.3). For 70 patients, CT was performed within the first week after symptom onset. The time interval between CT and RT-PCR was 2.3 days (SD 3.8). Ground-glass opacity was the most frequent feature occurring in almost all CTs (n = 116; 97 %). The second most frequent CT feature was consolidation which was seen on 93 CT scans (78 %). The crazy paving pattern was present on 23 CT scans (19 %) (▶ **Fig. 2**). Bronchial dilatation was seen on 31 (26 %) CT scans (▶ **Fig. 3**). Vessel enlargement was seen on 60 CT scans (50 %) (▶ **Fig. 4**). Curvilinear or band-like configuration of densities occurred on 50 CT scans (42 %) (▶ **Fig. 5**). A round shape of the opacification was observed on 46 CT scans (38 %) (▶ **Fig. 6**). An at least to some extent sharp margin of the pulmonary lesions was present on 96 CT scans (80 %) and a geographic shape on 36 CT scans (30 %) (▶ **Fig. 7**). Lymphadenopathy was detected on 41 CT scans (34 %). Pleural effusions were present on a minority of CT scans (n = 22, 18 %). Cavitations were not seen in either case. The lung was almost always bilaterally affected (n = 113; 94 %). The opacifications were predominantly located in the periphery of the lung and the posterior lung segments. The lower lobes were most often affected. The results are summarized in ▶ **Table 2**.

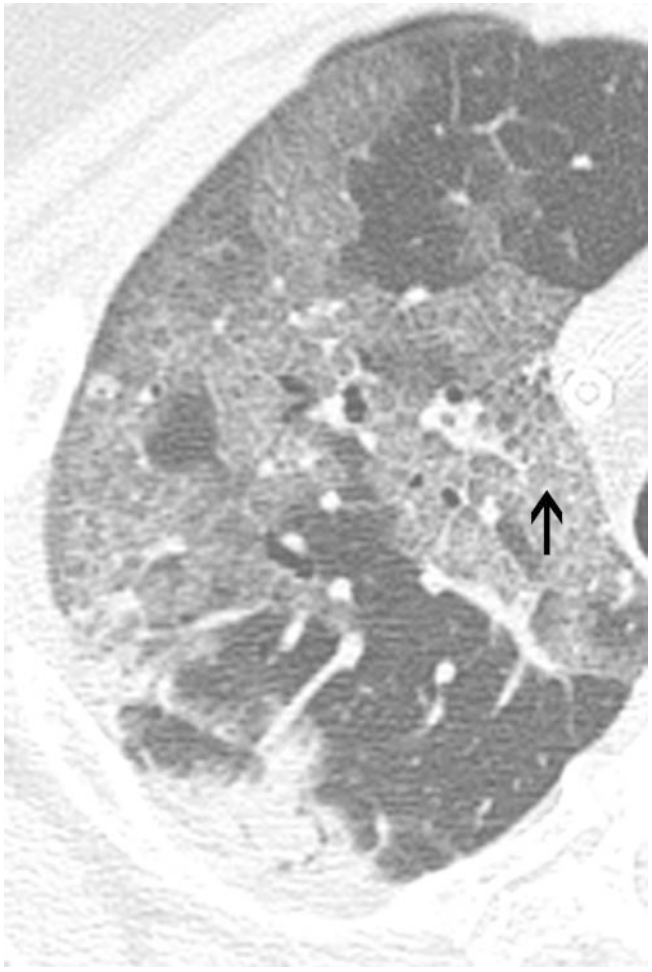

▶ **Fig. 2** Axial MPR of a thin-section CT scan of a patient with RT-PCR-proven COVID-19 pneumonia showing the crazy paving pattern: thickened interlobular septa and intralobular lines superimposed on a background of ground-glass opacity (arrow). The crazy paving pattern was present on 23 CT scans (19 %). Frequency of crazy paving increased highly significantly with an increasing extent of parenchymal opacification (2 %, 12 %, 44 %, respectively) and with duration of disease (10 %, 17 % 26 %, 37 %, respectively).

▶ **Abb. 2** Axiale MPR einer Dünnschicht-CT eines Patienten mit RT-PCR gesicherter COVID-19-Pneumonie. Unter anderem ist „crazy-paving" zu erkennen erkenntlich an verdickten interlobulären Septen und intralobulären Linien vor dem Hintergrund von Milchglas (Pfeil). Das crazy-paving war bei 23 CT-Scans (19 %) vorhanden. Die Häufigkeit des crazy-pavings nahm hochsignifikant mit dem Ausmaß der Verdichtungen (2 %, 12 % bzw. 44 %) und mit der Dauer der Erkrankung (10 %, 17 %, 26 % bzw. 37 %) zu.

▶ **Fig. 3** Axial MPR of a thin-section CT scan of a patient with RT-PCR-proven COVID-19 pneumonia and dilatation of the non-tapering bronchus with respect to the accompanying pulmonary artery (arrows). The term "dilatation" instead of "ectasis" was intentionally used in order to express that the pathology might be reversible. Bronchial dilatation was seen on 26 % of the CT scans and most often seen in the severe group (41 %).

▶ **Abb. 3** Axiale MPR einer Dünnschicht-CT eines Patienten mit RT-PCR gesicherter COVID-19-Pneumonie. Einige Bronchien sind dilatiert und verjüngen sich nicht im Verlauf (Pfeile). Der Begriff „Dilatation" anstelle von „Ektasie" wurde absichtlich verwendet, um auszudrücken, dass die Pathologie möglicherweise reversibel ist. Bei 26 % der CT-Scans wurde eine Dilatation von Bronchien gesehen, am häufigsten in der Gruppe der schwer betroffenen Patienten (41 %).

Subgroup analysis according to the extent of parenchymal opacification

GGO was present on nearly all CT scans independently of the extent of disease (mild: 91 %, moderate: 100 %, severe: 100 %). Differences were statistically significant ($p = 0.022$). Also, consolidation was frequently seen (63 %, 76 %, 95 %). The prevalence of consolidation increased significantly ($p < 0.0001$) with severity of parenchymal opacification. Moreover, the frequency of crazy paving increased highly significantly with increasing extent of parenchymal opacification (2 %, 12 %, 44 %, $p < 0.0001$). A round shape of GGO and consolidation was tended to be detected in the mild and moderate stages (41 % and 48 %, respectively) rather than in the severe stage (27 %) ($p = 0.181$). Sharp demarcation (at least to some extent) of opacifications with respect to the surrounding healthy tissue occurred frequently in all severity groups (70 %, 88 %, 85 %, $p = 0.061$). However, a geographic shape of the

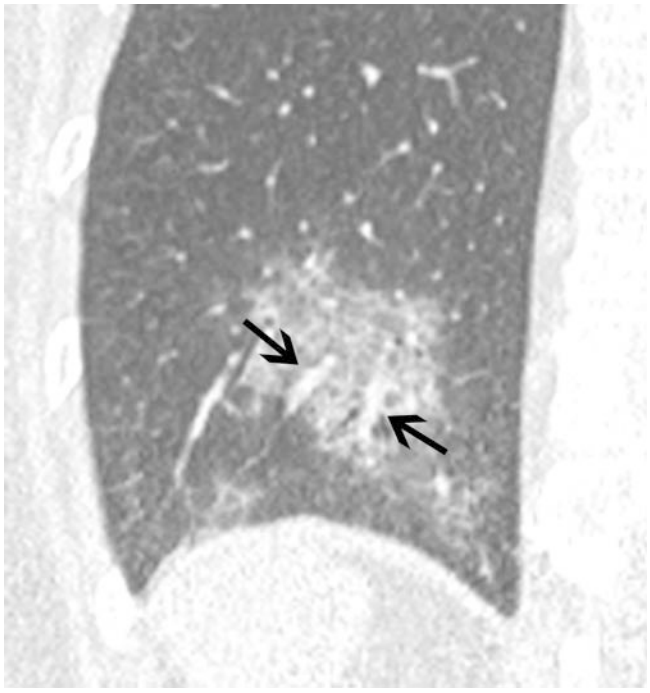

▶ **Fig. 4** Coronal MPR of a thin-section CT scan of a patient with RT-PCR-proven COVID-19 pneumonia and a dilated diameter of vessels within opacifications, clearly larger compared to vessels of the same generation in healthy lung tissue. Vessel enlargement was seen on 60 CT scans (50 %) and present in approximately the same proportion of patients in all extent groups (41 %, 55 %, 56 %, respectively).

▶ **Abb. 4** Koronare MPR einer Dünnschicht-CT eines Patienten mit RT-PCR gesicherter COVID-19-Pneumonie. Innerhalb der Milchglastrübung sind die Gefäße deutlich erweitert im Vergleich zu Gefäßen derselben Generation im gesunden Lungengewebe. Eine Gefäßerweiterung wurde bei 60 CT-Scans (50 %) gesehen und war in etwa gleich häufig bei allen drei Schweregraden an Parenchymverdichtungen vorhanden (41 %, 55 % bzw. 56 %).

lesions was seen significantly more often (p = 0.002) in the moderate (42 %) and severe (41 %) group compared to the mild group (11 %). Curvilinear/band-like lesions were seen significantly more often (p = 0.010) in the mild (50 %) and moderate (55 %) groups compared to the severe group (22 %). Bronchial dilatation was seen most often in the severe group (41 %) and less often in the mild (20 %) and moderate (15 %) groups (p = 0.023). Intralesional/perilesional vessel enlargement was present in approximately the same proportion of patients in all groups (41 %, 55 %, 56 %, p = 0.165). Pleural effusion (11 %, 9 %, 22 %) and lymphadenopathy (22 %, 30 %, 51 %) were seen significantly more often in the severe group (p = 0.006 and p = 0.004, respectively).

Bilateral involvement of the lungs was seen on nearly all CT scans in the mild stage (85 %), however, further increased in frequency in the moderate and severe stages (100 %, 100 %, p = 0.002). Opacifications were limited to one lung on only a small minority of CT scans with mild parenchymal involvement (11 %). None of the CT scans in the moderate or severe stage demonstrated unilateral disease (p = 0.010). The lower lobes were frequently involved already in the mild stage (RLL: 91 %, LLL: 85 %) with an

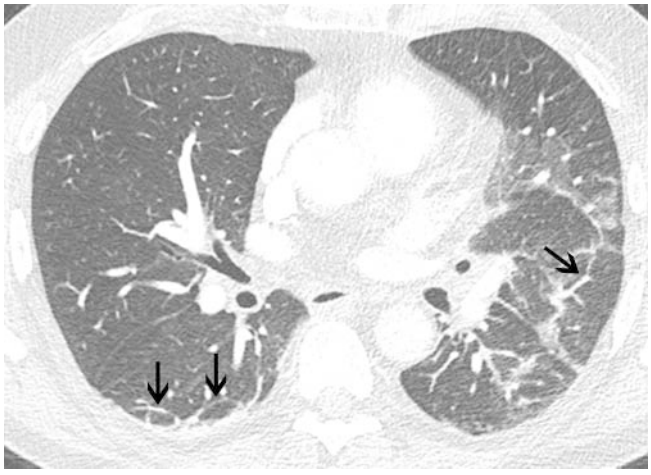

▶ **Fig. 5** Axial MPR of a thin-section CT scan of a patient with RT-PCR-proven COVID-19 pneumonia and a curvilinear/band-like shape of opacifications (arrows). Curvilinear or band-like configuration of densities occurred on 50 CT scans (42 %) and were seen significantly more often in the mild (50 %) and moderate (55 %) groups.

▶ **Abb. 5** Axiale MPR einer Dünnschicht-CT eines Patienten mit RT-PCR gesicherter COVID-19-Pneumonie. Die Verdichtungen sind bogig oder bandförmig konfiguriert (Pfeile). Dieser Befund trat bei 50 CT-Scans (42 %) auf und wurde signifikant häufiger in der mild (50 %) und moderat (55 %) betroffenen Gruppe beobachtet.

increasing percentage in the moderate and severe stages (RLL: 100 %, 100 %, p = 0.022; LLL: 100 %, 100 %, p = 0.002). Involvement of the three remaining lobes increased significantly with severity of disease (RML: 65 %, 97 %, 100 %, p < 0.001; RUL: 70 %, 100 %, 100 %, p < 0.001, LUL: 61 %, 100 %, 100 %, p < 0.001). Predominance of the lung core was observed in no cases. On the contrary, predominant affection of the lung periphery was seen on 87 % of CT scans in the mildly affected group. This percentage decreased significantly for the moderate (67 %) and severe groups (44 %) (p < 0.001). Correspondingly, the percentage of CT scans exhibiting diffuse distribution of opacifications in the axial plane increased from 24 % in the mild group to 45 % in the moderate group to finally 66 % in the severe group (p < 0.001). Only a small minority of patients with mild parenchymal involvement (4 %) demonstrated a predominance of opacifications in the anterior segments (moderate 0 %, severe 0 %, p = 0.110). For the remainder of patients, lung involvement dominated in the posterior segments in all stages (p = 0.424).

The results are summarized in ▶ **Table 2, 3**.

Subgroup analysis according to duration of disease

Symptom onset was not evaluable for 14 patients. Hence, 94 CT examinations were included in this subgroup analysis. Time interval between symptom onset and CT date was subclassified into four groups: 0–5 days (n = 21), 6–10 days (n = 35), 11–15 days (n = 19) and > 15 days (n = 19).

GGO was present in nearly all patients (98 %) independent of duration of disease (days 0–5: 92 %, days 6–10: 90 %, days 11–15: 100 %, > 15 days: 100 %, p = 0.059). By contrast, the frequency of

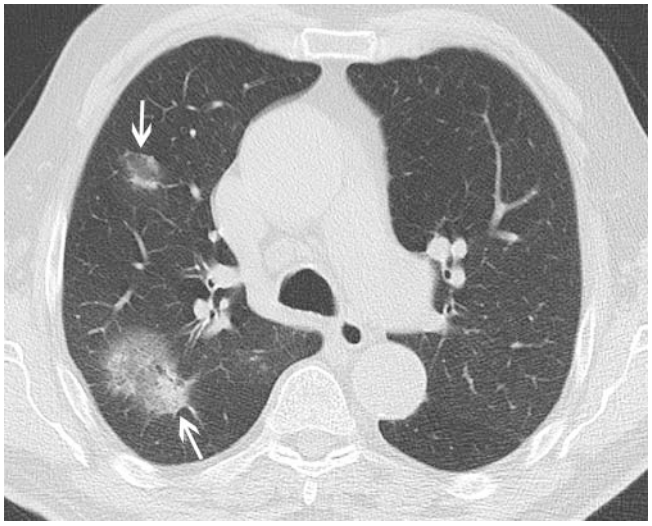

▶ **Fig. 6** Axial MPR of a thin-section CT scan of a patient with RT-PCR-proven COVID-19 pneumonia and a round shape of opacities (arrows). A round shape of the opacification was observed on 46 CT scans (38 %) and tended to be detected in the mild and moderate stages (41 % and 48 %, respectively) rather than in the severe stage (27 %).

▶ **Abb. 6** Axiale MPR einer Dünnschicht-CT eines Patienten mit RT-PCR gesicherter COVID-19-Pneumonie. Die Verdichtungen sind rundlich konfiguriert (Pfeile). Eine runde Form der Verdichtungen wurde bei 46 CT-Scans (38 %) gesehen und war häufiger in den mild und moderat betroffenen Fällen (41 % bzw. 48 %) als in den schweren Stadien (27 %) vorhanden.

consolidation (62 %, 66 %, 95 %, 89 %) and especially crazy paving (10 %, 17 % 26 %, 37 %) increased significantly with the duration of disease (p = 0.007 and p = 0.025, respectively). Also, bronchial dilatation (19 %, 20 %, 21 %, 47 %, p = 0.047), the presence of nodules (5 %, 3 %, 21 %, 21 %, p = 0.022), and a curvilinear/band-like configuration of opacifications (10 %, 51 %, 42 %, 42 %, p = 0.096) were seen more often later during the course of disease. A round (48 %, 54 %, 21 %, 21 %, p = 0.014) or geographic (43 %, 34 %, 26 %, 16 %, p = 0.052) shape of opacifications was less conspicuous in the later phases of the disease. A sharp margin, however, was continuously present in a high percentage of cases (67 %, 89 %, 79 %, 74 %, p = 0.874). Enlargement of vessels within or around lesions demonstrated an undulating frequency (57 %, 37 %, 58 %, 42 %, p = 0.715) during the course of disease. Lymphadenopathy (29 %, 31 %, 42 %, 53 %, p = 0.080) and pleural effusions (19 %, 6 %, 21 %, 32 %, p = 0.124) were present more often in the later stages.

Unilateral involvement of the lungs was seen only in a minority of patients and limited to the early stages of disease (14 %, 6 %, 0 %, 0 %, p = 0.031). Analysis of involvement of lung lobes revealed that both lower lobes were involved from the very beginning of the disease in most cases (RLL 86 %, 100 %, 100 %, 95 %, p = 0.217; LLL 90 %, 91 %, 95 %, 100 %, p = 0.185). The frequency of appearance of opacifications in the right middle lobe and right upper lobe was already high in the early disease stages and further increased with evolving disease (RML 76 %, 86 %, 89 %, 95 %, p = 0.088; RUL 81 %, 91 %, 84 %, 89 %, p = 0.638). The left upper

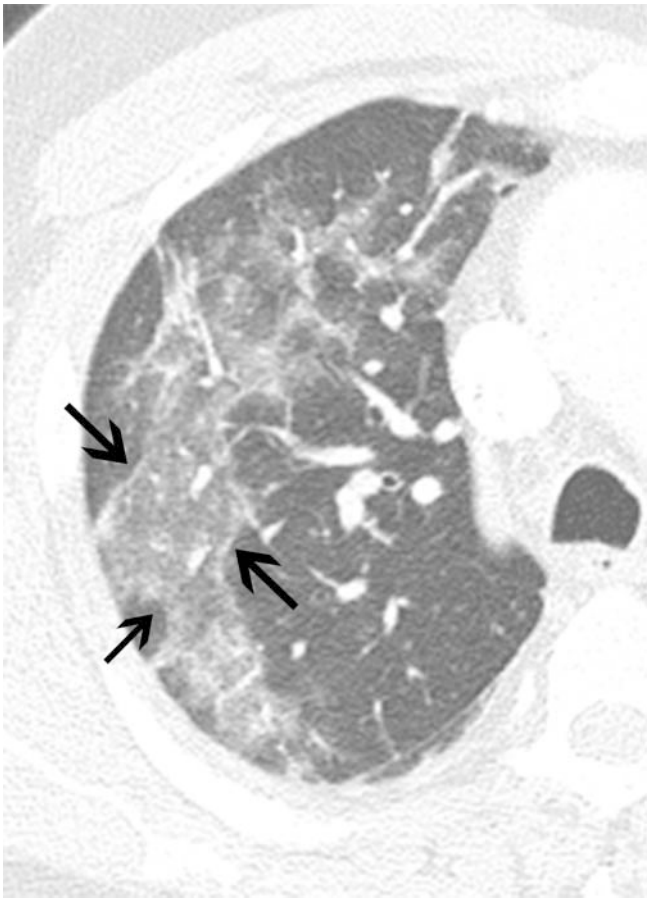

▶ **Fig. 7** Axial MPR of a thin-section CT scan of a patient with RT-PCR-proven COVID-19 pneumonia. Opacities have a geographic shape and at least to some extent have sharp margins with respect to the surrounding healthy lung tissue (arrows). An at least to some extent sharp margin of the pulmonary lesions was present on 96 CT scans (80 %) and a geographic shape on 36 CT scans (30 %). A geographic shape of the lesions was seen significantly more often in the moderate (42 %) and severe (41 %) groups.

▶ **Abb. 7** Axiale MPR einer Dünnschicht-CT eines Patienten mit RT-PCR gesicherter COVID-19-Pneumonie. Die Verdichtungen zeigen eine geographische Konfiguration und weisen anteilig eine scharfe Berandung auf (Pfeile). Eine scharfe Begrenzung der Verdichtungen war auf 96 CT Scans (80 %) erkennbar und eine geografische Konfiguration auf 36 CT-Scans (30 %). Die geographische Konfiguration wurde signifikant häufiger in der moderat (42 %) und schwer betroffenen (41 %) Gruppe beobachtet.

lobe was affected only moderately often in the early stage (62 %). However, with a longer duration of disease, the frequency of involvement increased continuously (89 %, 89 %, 95 %, p = 0.009). The location of lesions predominantly in the lung periphery was most distinct in the early disease stages with decreasing conspicuity in the late phase (67 %, 77 %, 68 %, 37 %, p = 0.033). Accordingly, diffuse distribution in the axial plane was seen slightly more often in late phase images compared to early phase images (43 %, 37 %, 37 %, 58 %). However, this difference did not reach statistical significance (p = 0.352). Predominance of opacifications in the posterior segments was appreciable through the entire course of

▶ **Table 2** Frequency of CT features as a function of extent of parenchymal opacifications.

	total (%) n = 120	mild (%) n = 46	moderate (%) n = 33	severe (%) n = 41	p-value
signs					
ground glass opacity	116 (97)	42(91)	33 (100)	41 (100)	0.022
consolidation	93 (78)	29 (63)	25 (76)	39 (95)	< 0.001
crazy paving	23 (19)	1 (2)	4 (12)	18 (44)	< 0.001
bronchial dilatation	31 (26)	9 (20)	5 (15)	17 (41)	0.023
nodules	14 (12)	2 (4)	3 (9)	9 (22)	0.012
cavitations	0 (0)	0 (0)	0 (0)	0 (0)	
vessel enlargement	60 (50)	19 (41)	18 (55)	23 (56)	0.165
shape and margin					
round shape	46 (38)	19 (41)	16 (48)	11 (27)	0.181
sharp margins	96 (80)	32 (70)	29 (88)	35 (85)	0.061
geographic shape	36 (30)	5 (11)	14 (42)	17 (41)	0.002
curvilinear/bandlike	50 (42)	23 (50)	18 (55)	9 (22)	0.010
extrapulmonary findings					
lymphadenopathy	41 (34)	10 (22)	10 (30)	21 (51)	0.004
pleural effusions	22 (18)	5 (11)	3 (9)	14 (34)	0.006

▶ **Table 3** Distribution of CT features as a function of extent of parenchymal opacifications.

distribution	total (%) n = 120	mild (%) n = 46	moderate (%) n = 33	severe (%) n = 41	p-value
unilateral	5 (4)	5 (11)	0 (0)	0 (0)	0.010
bilateral	113 (94)	39 (85)	33 (100)	41 (100)	0.002
right upper lobe	106 (88)	32 (70)	33 (100)	41 (100)	< 0.001
right middle lobe	103 (86)	30 (65)	32 (97)	41 (100)	< 0.001
right lower lobe	116 (97)	42 (91)	33 (100)	41 (100)	0.022
left upper lobe	102 (85)	28 (61)	33 (100)	41 (100)	< 0.001
left lower lobe	113 (94)	39 (85)	33 (100)	41 (100)	0.002
predominantly peripheral	80 (67)	40 (87)	22 (67)	18 (44)	< 0.001
predominantly central	0 (0)	0 (0)	0 (0)	0 (0)	
diffuse	53 (44)	11 (24)	15 (45)	27 (66)	< 0.001
predominantly anterior	2 (2)	2 (4)	0(0)	0 (0)	0.110
predominantly posterior	94 (78)	38 (83)	25 (76)	31 (76)	0.424

disease (81 %, 80 %, 74 %, 79 %, p = 0.747). The correlation of degree of parenchymal involvement with disease duration demonstrated significantly increasing extent of opacifications with evolving disease (mild: 52 %, 43 %, 32 %, 16 %, p = 0.012; moderate: 33 %, 40 %, 21 %, 11 %, p = 0.042; severe: 14 %, 17 %, 47 %, 74 %, p < 0.001).

The results are summarized in ▶ **Table 4, 5**.

Discussion

The standard of reference for the diagnosis of COVID-19 is RT-PCR. However, the reported sensitivities of RT-PCR range between 42 % and 83 % depending on several factors like viral load at the sample site, quality of the specimen, and test quality (10). Moreover, it takes hours to days before RT-PCR results are available. Authorities in China used chest CT to fill this gap. The rationale for this strategy was that, on the one hand, the sensitivity of

▶ **Table 4** Frequency of CT features as a function of duration of disease.

CT Feature	total n = 94	0–5 days n = 21	6–10 days n = 35	11–15 days n = 19	> 15 days n = 19	p-value
signs						
ground glass opacity	92 (98)	19 (90)	35 (100)	19 (100)	19 (100)	0.059
consolidation	71 (76)	13 (62)	23 (66)	18 (95)	17 (89)	0.007
crazy paving	20 (21)	2 (10)	6 (17)	5 (26)	7 (37)	0.025
bronchial dilatations	24 (26)	4 (19)	7 (20)	4 (21)	9 (47)	0.047
nodules	10 (11)	1 (5)	1 (3)	4 (21)	4 (21)	0.022
cavitations	0 (0)	0 (0)	0 (0)	0 (0)	0 (0)	
vessel enlargement	44 (47)	12 (57)	13 (37)	11 (58)	8 (42)	0.715
shape and margin						
round shape	37 (39)	10 (48)	19 (54)	4 (21)	4 (21)	0.014
sharp margin	74 (79)	14 (67)	31 (89)	15 (79)	14 (74)	0.874
geographic shape	29 (31)	9 (43)	12 (34)	5 (26)	3 (16)	0.052
curvilinear/bandlike	36 (38)	2 (10)	18 (51)	8 (42)	8 (42)	0.096
extrapulmonary findings						
lymphadenopathy	35 (37)	6 (29)	11 (31)	8 (42)	10 (53)	0.080
pleural effusions	16 (17)	4 (19)	2 (6)	4 (21)	6 (32)	0.124

▶ **Table 5** Distribution of CT features as a function of duration of disease.

distribution	total n = 94	0–5 days n = 21	6–10 days n = 35	11–15 days n = 19	> 15 days n = 19	p-value
unilateral	5 (5)	3 (14)	2 (6)	0 (0)	0 (0)	0.031
bilateral	87 (93)	17 (81)	32 (91)	19 (100)	19 (100)	0.012
right upper lobe	82 (87)	17 (81)	32 (91)	16 (84)	17 (89)	0.638
right middle lobe	81 (86)	16 (76)	30 (86)	17 (89)	18 (95)	0.088
right lower lobe	90 (96)	18 (86)	35 (100)	19 (100)	18 (95)	0.217
left upper lobe	79 (84)	13 (62)	31 (89)	17 (89)	18 (95)	0.009
left lower lobe	88 (94)	19 (90)	32 (91)	18 (95)	19 (100)	0.185
predominantly peripheral	61 (65)	14 (67)	27 (77)	13 (68)	7 (37)	0.033
predominantly central	0 (0)	0 (0)	0 (0)	0 (0)	(0)	
diffuse distribution	40 (43)	9 (43)	13 (37)	7 (37)	11 (58)	0.352
predominantly anterior	2 (2)	0 (0)	2 (6)	0 (0)	0 (0)	0.602
predominantly posterior	74 (79)	17 (81)	28 (80)	14 (74)	15 (79)	0.747
extent of opacifications						
mild	35 (37)	11 (52)	15 (43)	6 (32)	3 (16)	0.012
moderate	27 (29)	7 (33)	14 (40)	4 (21)	2 (11)	0.042
severe	32 (34)	3 (14)	6 (17)	9 (47)	14 (74)	< 0.001

chest CT is high (around 95 %) and was reported to be even higher than RT-PCR [11, 12]. On the other hand, the literature showed that CT is not only sensitive but also suggestive for the diagnosis in many cases. A combination of multifocal bilateral GGO, consolidation, and crazy paving pattern located in the periphery of the posterior segments predominantly of the lower lung lobes was reported to be characteristic for COVID-19 pneumonia in chest CT. Vessel enlargement within or around the opacifications was

shown to be a phenomenon which seems to enable differentiation of COVID-19 pneumonia from other types of pneumonia [13]. In principle, CT morphology in our cohort is in accordance with previous reports. Despite the fact that CT morphology seems to be characteristic, the specificity of chest CT for COVID-19 pneumonia is dismal with reported numbers as low as 37 % [10].

Obviously, the specificity of CT for any disease depends on the uniqueness of the CT morphology. In the case of viral pneumonias, no such pathognomonic features exist. However, a combination of several suggestive and frequently occurring signs and distribution patterns would be helpful to increase specificity. The analysis of the CT morphology of COVID-19 pneumonia in our cohort revealed that the frequency of CT features was highly dependent on disease extent and duration. For example, crazy paving pattern is reported to be characteristic for COVID-19 pneumonia. However, in our cohort crazy paving was detectable on a substantial percentage of CT scans only late in the course of disease and in patients with extensive parenchymal involvement. Conversely, a round shape of opacifications was lost in the late phase of disease. Lymphadenopathy and pleural effusion were shown in the literature to be a rather seldom feature of COVID-19 pneumonia. However, in our cohort this only applied to the early and mild stages of disease. Later on, and with an increasing degree of opacifications, the percentage of patients presenting with lymphadenopathy and pleural effusions was substantial. Analysis of distribution of lesions within the lung revealed that the predominant involvement of the lung periphery (which has been described as characteristic for COVID-19 pneumonia) is significantly better appreciable when the disease extent is mild compared to severe.

Considering our results, it is obvious that the specificity of CT for COVID-19 pneumonia is low when the identical compound of signs and distribution patterns is applied for the entire course of the disease and all degrees of parenchymal opacification. We hypothesize that the specificity of chest CT might be better when tailoring the expected findings to the duration and extent of disease. We therefore propose the following diagnostic strategy: In the early phase of disease (day 0–5 after symptom onset) COVID-19 pneumonia is characterized by GGO and minor consolidation. Crazy paving, lymphadenopathy, and pleural effusion are present in a minority of patients. The opacifications can have a round shape and to some extent sharp margins and a geographic configuration. Lesions are found bilaterally in the periphery of all lobes, predominantly in the posterior segments. The left upper lobe might be spared. Between day 6 and 15 after symptom onset, the frequency of consolidation and especially crazy paving increases. The round and geographic shape of lesions fades. A curvilinear shape of opacifications is seen increasingly often. Still the lesions have partially sharp margins. All lobes are involved with predominance in the periphery of the lung. Beyond day 15, crazy paving, lymphadenopathy, and pleural effusion are present in a substantial percentage of patients. As a new sign, bronchial dilatation occurs. The opacifications still have partially sharp margins. Accentuation of lesions in the periphery of the lung is not as conspicuous as before and is replaced by a diffuse distribution pattern.

Our study has limitations. All included patients were RT-PCR-positive for SARS-CoV 2. Thus, our data did not allow investigation of the sensitivity of CT compared to RT-PCR or the specificity of CT for COVID-19 pneumonia. The proportion of patients with severely involved lung parenchyma was relatively high. This was probably due to the fact that both hospitals were tertiary care institutions with one of them being the regional center for critically ill patients. The correlation of most severe parenchymal involvement in the late phase of disease is probably due to the same circumstance. Hence, the observed dynamic might apply more to seriously ill patients than to mild courses. Another limiting factor of our study is the fact that differences in patient management such as treatment in the ICU, ventilation parameters, and ECMO therapy were not taken into account. Hence, a possible influence of patient management on CT morphology could not be evaluated. Patient outcomes were not yet available at the time of submission of this article.

Conclusion

We present a cohort of 108 patients with RT-PCR-proven COVID-19 pneumonia who underwent chest CT. The CT morphology in this cohort was in accordance with published data. However, the prevalence and conspicuity of CT features changed during the course of disease and depending on the severity of parenchymal involvement. Thus, radiologists should take into account the time interval between symptom onset and the date of CT examination and the severity of disease when discussing the likelihood of COVID-19 pneumonia based on CT morphology. Further prospective studies are warranted to confirm these findings.

CLINICAL RELEVANCE

- CT can be a helpful supplement for the diagnosis and follow-up of COVID-19 pneumonia.
- However, the frequency of CT features and the pattern of parenchymal involvement of COVID-19 pneumonia varies depending on the duration and the extent of the disease.
- Radiologists should be aware of the different faces COVID-19 pneumonia.

Funding

The authors state that this work has not received any funding.

Ethics approval

This retrospective study was approved by the institutional ethics committee. All procedures performed in studies involving human participants were in accordance with the ethical standards of the institutional and/or national research committee and with the 1964 Helsinki declaration and its later amendments or comparable ethical standards. Written informed consent was waived.

Author Contributions

J.S. and O.W.H designed the study. J.S., S.M., C.K., H.K., C.M. were responsible for data collection. F.Z. performed the statistical analyses, J.S. and O.W.H. prepared the manuscript, which was critically revised and amended by F.P., G.S., J.R., B.P., C.S., N.Z..J. S. is the guarantor of the paper, taking responsibility for the integrity of the work as whole from inception to published article.

Conflicts of interest

The authors of this manuscript declare no relationships with any companies, whose products or services may be related to the subject matter of the article.

References

[1] Shi H, Han X, Jiang N et al. Radiological findings from 81 patients with COVID-19 pneumonia in Wuhan, China: a descriptive study. Lancet Infect Dis 2020; 20: 425–434

[2] Ng MY, Lee EY, Yang J et al. Imaging Profile of the COVID-19 Infection: Radiologic Findings and Literature Review. Radiol Cardiothorac Imaging 2020; 2: e200034. Im Internet: http://pubs.rsna.org/doi/10.1148/ryct.2020200034

[3] Li K, Wu J, Wu F et al. The Clinical and Chest CT Features Associated with Severe and Critical COVID-19 Pneumonia. Investigative Radiology 2020; 55: 327–331

[4] Han R, Huang L, Jiang H et al. Early Clinical and CT Manifestations of Coronavirus Disease 2019 (COVID-19) Pneumonia. American Journal of Roentgenology 2020; 215: 338–343. doi:10.2214/AJR.20.22961

[5] Chung M, Bernheim A, Mei X et al. CT imaging features of 2019 novel coronavirus (2019-NCoV). Radiology 2020; 295: 202–207

[6] Caruso D, Zerunian M, Polici M et al. Chest CT Features of COVID-19 in Rome, Italy. Radiology 2020; 296: E79–E85. doi:10.1148/radiol.2020201237. Epub 2020 Apr 3

[7] Revel MP, Parkar AP, Prosch H et al. COVID-19 patients and the radiology department – advice from the European Society of Radiology (ESR) and the European Society of Thoracic Imaging (ESTI). Eur Radiol 2020; 30: 4903–4909. doi:10.1007/s00330-020-06865-y. Epub 2020 Apr 20

[8] Simpson S, Kay FU, Abbara S et al. Radiological Society of North America Expert Consensus Statement on Reporting Chest CT Findings Related to COVID-19. Endorsed by the Society of Thoracic Radiology, the American College of Radiology, and RSNA. Radiol Cardiothorac Imaging 2020; 2: e200152

[9] Prokop M, van Everdingen W, van Rees VellingaT et al. CO-RADS – A categorical CT assessment scheme for patients with suspected COVID-19: definition and evaluation. Radiology 2020; 296: E97–E104. doi:10.1148/radiol.2020201473. Epub 2020 Apr 27

[10] Kim H, Hong H, Yoon SH. Diagnostic Performance of CT and Reverse Transcriptase-Polymerase Chain Reaction for Coronavirus Disease 2019: A Meta-Analysis. Radiology 2020; 296: E145–E155. doi:10.1148/radiol.2020201343. Epub 2020 Apr 17

[11] Fang Y, Zhang H, Xie J et al. Sensitivity of Chest CT for COVID-19: Comparison to RT-PCR. Radiology 2020; 296: E115–E117. doi:10.1148/radiol.2020200432. Epub 2020 Feb 19

[12] Ai T, Yang Z, Hou H et al. Correlation of Chest CT and RT-PCR Testing in Coronavirus Disease 2019 (COVID-19) in China: A Report of 1014 Cases. Radiology 2020; 296: E32–E40. doi:10.1148/radiol.2020200642. Epub 2020 Feb 26

[13] Bai HX, Hsieh B, Xiong Z et al. Performance of radiologists in differentiating COVID-19 from viral pneumonia on chest CT. Radiology 2020; 296: E46–E54. doi:10.1148/radiol.2020200823. Epub 2020 Mar 10